A Novel ω-Helical Conformation in Poly(N^{ϵ}-(*p*-halobenzoyl)-L-ornithine)s

Shintaro Sasaki* and Yoshimu Iwanami

Department of Polymer Chemistry, Tokyo Institute of Technology, Ookayama, Meguro-ku, Tokyo, 152 Japan. *Received March 7, 1988; Revised Manuscript Received March 14, 1988*

ABSTRACT: A novel ω-helical conformation with the unit height p = 1.42 Å was found for the heat-treated forms of poly(N^{ϵ}-(*p*-halobenzoyl)-L-ornithine)s [(–NHC$^{\alpha}$HRC′O–)$_n$, R = –$(CH_2)_3$–N^{ϵ}HCOC_6H_4X] with the halogen atom X = F, Cl, and Br. The unit height is substantially greater than 1.325 Å reported for the ω-helix of poly(β-benzyl-L-aspartate). These ω-forms crystallize in the isomorphous orthorhombic structure with space group $P2_12_12_1$. The main chain assumes a 4_{13} helix conformation with nonplanar peptide units. The side chains take two distinctive conformations alternately in accord with the 2_1 crystal symmetry. Intra- and intermolecular hydrogen bonds are formed between the amide groups of the side chains. On the basis of this structure, the adequacy of the ribbon model, which has been used to describe the helical conformations of polypeptides, is examined.

Introduction

Synthetic polypeptides exist in various helical conformations with the intramolecular hydrogen bonds of the (N_j—H_j···O_i=C′$_i$) type.[1-3] Most of the L enantiomers form the right-handed α-helix (j = 5). The standard α-helix (3.6_{13}) is characterized by a unit height p = 1.50 Å (axial translation per residue) and the unit twist t = 100° (angular separation between residues). Poly(β-benzyl-L-aspartate) (PBLA) forms a left-handed helix (t < 0) and is therefore exceptional. Its α-helix is transformed at ~160 °C into the ω-helix (4_{13}) (j = 5) with p = 1.325 Å.[4] In this paper, we define the ω-helix as having four residues per turn (i.e., $|t| \equiv 90°$). The values of p of the ω-helices reported so far are 1.30 Å for poly(β-(*p*-chlorobenzyl)-L-aspartate) (*p*-Cl-PBLA),[5] 1.39 Å for poly(*S*-(benzylthio)-L-cysteine),[6] and 1.40 Å for poly(L-phenylalanine).[7,8] Poly(β-phenethyl-L-aspartate) exists as a π-helix (4.25_{16}) (j = 6) with p = 1.17 Å and t = –84.7°.[9] Recently, poly(α-aminoisobutyric acid) was shown to exist as a 3_{10} helix ($|t| \equiv 120°$, j = 4) with $p \sim 1.96$ Å.[10,11]

A correlation between unit height p and unit twist t is evident in Figure 1. Fraser et al. regarded the polypeptide chain as a ribbon of width w wrapped around a cylinder of radius equal to the radial coordinate of C$^{\alpha}$. They derived a relationship between p and t in terms of w and the distance d between successive C$^{\alpha}$ atoms.[3,12] It can be shown that the p–t relationship is simplified by the pleated-ribbon model illustrated in Figure 2 as follows:

$$p^4 - d^2p^2 + (wdt/2\pi)^2 = 0 \qquad (1)$$

This equation expresses almost the same p–t relationship as that of Fraser et al. If the peptide-bond torsion angle ω(C′–N) is 180° (trans), $d = d_s$ = 3.80 Å with the standard dimensions of bond lengths and bond angles given by Corey and Pauling (Figure 5).[13] If w is chosen so that the standard α-helix is a solution of eq 1 (namely, $w = w_s$ = 4.962 Å), the p–t relationship is given by the solid line in Figure 1. When ω is changed from 170° to 190°, the value of d varies only between 3.793 and 3.800 Å. Leach et al.[14] tabulated the variations of d = 3.71–3.85 Å in simple compounds. According to Fraser et al.,[12] an increase in d was accompanied by a decrease in w

$$w = w_s = -0.8(d - d_s) \qquad (2)$$

Inserting d = 3.71 and 3.85 Å, we obtain w = 5.034 and 4.922 Å, respectively. The curves for these limiting values are shown by the broken lines in Figure 1. Most of the α-helices fall in the small range admitted by the ribbon model. However, some ω-helices are beyond the scope. The departure is still greater for the ω-helix found in the present work (mark 6 in Figure 1) for the heat-treated forms of poly(N^{ϵ}-(*p*-halobenzoyl)-L-ornithine)s (PXBO) with X = F, Cl, and Br.

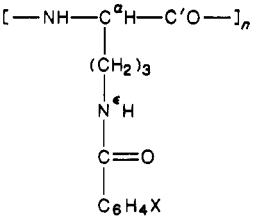

This indicates that the ribbon width is not given by eq 2 or that the ribbon model itself is an oversimplification of the problem. In this paper, the structure of the novel ω-form is analyzed by X-ray diffraction, and the adequacy of the ribbon model is discussed.

Experimental Section

Samples. The PXBO polymers with X = H, F, Cl, and Br (namely, PHBO, PFBO, PClBO, and PBrBO, respectively) were synthesized by the *N*-carboxy anhydride method using triethylamine as the initiator in tetrahydrofuran (THF). They were recovered by precipitation with methanol and identified by their NMR spectra. Optical rotatory dispersion spectra were measured for the solutions in *N*,*N*-dimethylformamide with a Jasco J-20 spectropolarimeter. The Moffitt-Yang b_0 parameters are in the range from –560 to –640, supporting the right-handed helical conformation.

The films of PHBO, PClBO, and PBrBO were prepared by evaporating the solvent THF at room temperature, while PFBO was obtained as a powder (probably owing to the low molecular weight). Densities of the films were determined at 25 °C by the flotation method in carbon tetrachloride–cyclohexane mixtures. The thermograms were recorded by differential scanning calorimetry (DSC) at a scanning rate of 10 deg/min with a Perkin-Elmer DSC Model II instrument.

X-ray Diffraction. Wide-angle X-ray diffraction patterns were taken with Ni-filtered Cu Kα radiation by using a flat-plate camera and a cylindrical camera. The oriented specimens of PHBO, PClBO, and PBrBO were prepared by stroking the concentrated solutions onto glass plates. The meridional reflections were recorded by tilting the oriented samples from the normal to the incident beam. The reflection spacings were calibrated against the 111 reflection of silicon powder sprinkled over specimens. The intensities were measured by scanning the photographs with a microphotometer and corrected for the Lorentz–polarization factors.

Infrared (IR) Absorption. The IR spectra of the films prepared on KRS plates were recorded with a Jasco DS-701G grating spectrophotometer. Dichroism was measured for the oriented films of PClBO and PBrBO. The direction perpendicular to the *p*-halophenyl plane was determined from the dichroic ratio of the bands at ~840 cm^{-1} assigned to the out-of-plane C–H

0024-9297/88/2221-3389$01.50/0

Table I
Crystallographic Data

polymer (helix)	cryst system, space group	lattice const,[a] Å	N^b	density, g cm^{-3} obsd	density, g cm^{-3} calcd
PHBO (α)	hexagonal	a = 15.0, P = 5.4, p = 1.47	1	1.25	1.27
PFBO (ω)	orthorhombic, $P2_12_12_1$-D_2^4	a = 23.8, b = 18.7, p = 1.42	2		(1.24)
PClBO (ω)	orthorhombic, $P2_12_12_1$-D_2^4	a = 24.1, b = 18.5, c = 5.68, p = 1.42	2	1.32	1.33
PBrBO (ω)	orthorhombic, $P2_12_12_1$-D_2^4	a = 24.6, b = 18.4, c = 5.68, p = 1.42	2	1.52	1.54

[a] P, helix pitch; p, unit height. [b] N, number of helices per unit cell.

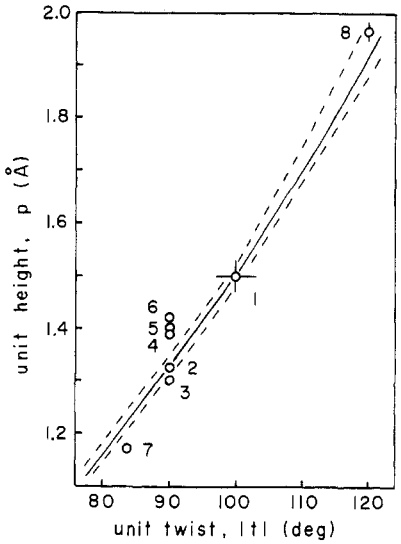

Figure 1. Correlation between unit height p and unit twist t of helical polypeptides. (1) The α-helical region;[3] (2) PBLA;[4] (3) p-ClPBLA;[5] (4) poly(*S*-(benzylthio)-L-cysteine);[6] (5) poly(L-phenylalanine);[7,8] (6) poly[(p-halobenzoyl)-L-ornithine]s (this work); (7) poly(β-phenethyl-L-aspartate);[9] (8) poly(α-aminoisobutyric acid).[10,11] Full line, a correlation offered by the pleated-ribbon model (Figure 2) with d = 3.80 Å, w = 4.962 Å; broken line (upper), d = 3.71 Å, w = 5.034 Å; broken line (lower), d = 3.85 Å, w = 4.922 Å.

bending. The angle θ between the transition moment and the helix axis was calculated from the dichroic ratio $R_d(\parallel/\perp)$ by

$$R_d(\parallel/\perp) = (2\cos^2\theta + g)/(\sin^2\theta + g) \quad (3)$$

where $g = (2/3)(1-f)/f$ and f is the orientational order parameter of the film.[3,15] The f has generally been determined from the dichroic ratio of the amide A or II band.[16-19] In the present case, these bands are overlapped for the main-chain and side-chain amide groups. Then the values of f were assumed to equal those of the films used for X-ray diffraction and determined to be 0.68 (PClBO) and 0.82 (PBrBO). It can be shown that uncertainties in f and R_d do not cause significant error in θ.

Results

Modifications. 1. PHBO. The X-ray diffraction pattern and the IR spectrum did not change under heat treatment in the temperature range below 200 °C. The equatorial reflections were indexed by a hexagonal unit cell with the lateral size a = 15.0 Å (Table I). The helix pitch P was estimated to be 5.4 Å from the spacing of the strong nonequatorial layer line. A meridional reflection was observed with spacing of 1.47 Å corresponding to the unit height p. Since P/p = 3.67, PHBO exists in the slightly distorted α-helical conformation.

2. PFBO. The powder sample as cast showed several broad reflections explained by the hexagonal unit cell of a ~16 Å. The crystallinity was rarely increased by heat treatments at 200 °C, and no transition was detected by DSC. However, a highly crystalline sample was in one instance obtained, although the reason was not clear. The diffraction pattern (Figure 3a) was similar to those of the annealed PClBO and PBrBO. This suggests that the

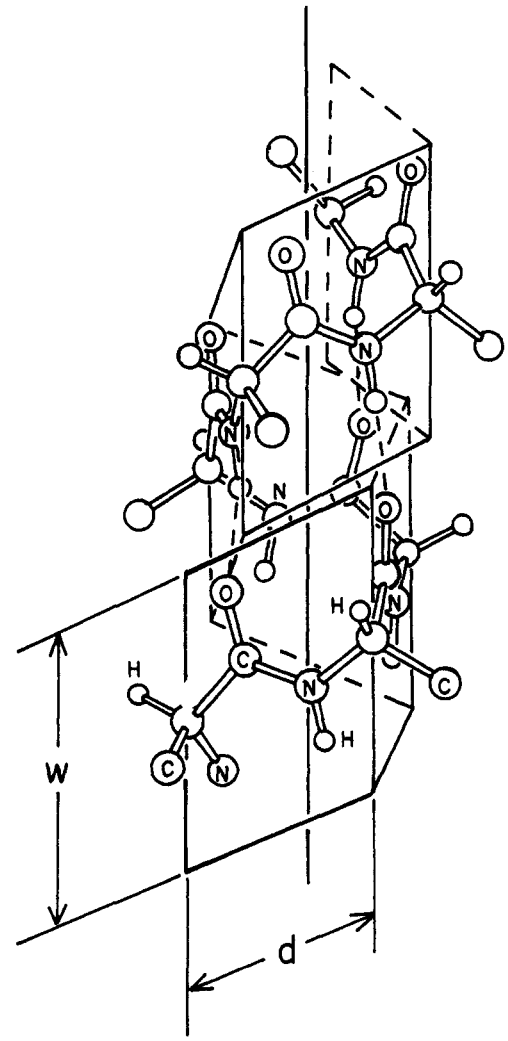

Figure 2. Pleated-ribbon model for helical conformations of synthetic polypeptides: d, C^α–C^α distance; w, ribbon width.

structures are isomorphous. By referring to the fiber patterns of PClBO and PBrBO, the reflections of PFBO were indexed by an orthorhombic unit cell (Table I). The lateral size indicates that two helices pass through the unit cell. The fiber identity distance c could not be determined. The annealed samples were mixtures of the hexagonal and orthorhombic forms. The conformational difference between these two forms was suggested from the IR data (Figure 4 and Table II).

3. PClBO. The crude precipitate and the film prepared by evaporating the solvent (THF) slowly through the liquid-crystalline state exhibited a DSC exotherm of ~1.8 cal/g at ~160 °C. The molecular conformation was originally α-helical, since the oriented film exhibited a meridional reflection at 1.49 Å. The film annealed at 200 °C (above the transition temperature) was highly crystalline (Figure 3b). The reflection spacings were explained by an orthorhombic unit cell with dimensions listed in Table I. A meridional reflection corresponding to p was observed

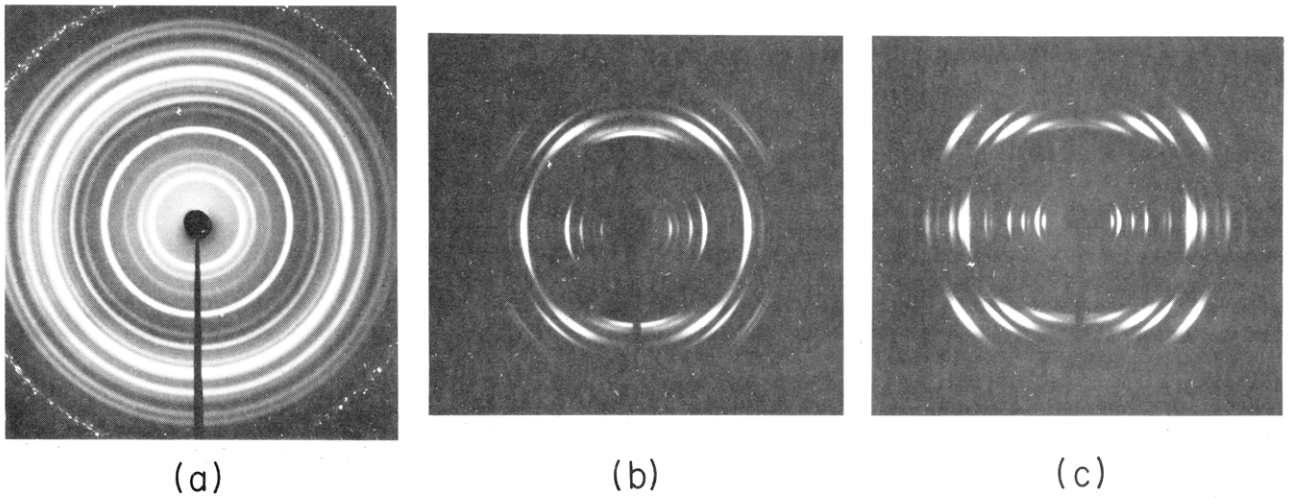

Figure 3. X-ray diffraction patterns of the ω-forms: (a) PFBO (powder), (b) PClBO (oriented), (c) PBrBO (oriented).

Table II
Frequencies of Characteristic Amide-Group Vibrations

		band positn,[a] cm^{-1}			
polymer	helix	amide A	amide I	amide II	amide V
PHBO	α	3290	1654	1547	~620
PFBO	α	3285	~1655	1550	~625
	ω	3300	1668	1550	625
			~1650	1533	605
PClBO and PBrBO	α	3300 (⊥)	~1650	~1545 (⊥)	~625 (⊥)
		3280 (∥)			
	ω	3300 (∥)	1660	1550 (⊥)	625 (⊥)
		3290 (⊥)	1640	1530 (⊥)	608 (⊥)

[a] The electric vector is parallel (∥) and perpendicular (⊥) to the oriented direction.

at 1.42 Å. Because of $c/p = 4$, the molecular conformation is ω-helical. The observed density indicates that two helices pass through the unit cell.

The transition from α to ω was irreversible in the solid state. The reverse transition occurred when the ω form was immersed in methanol for several hours and dried again. The methanol-treated film reproduced the original X-ray and IR patterns as well as the exothermic transition from α to ω.

The film prepared by evaporating the solvent quickly from the dilute solution did not exhibit the exothermic transition. The diffraction pattern was poor and not improved by heat treatments. On the other hand, the IR spectral changes suggested that the conformational transition from α to ω took place by heat treatments. This is discussed later.

4. PBrBO. The properties were similar to those of PClBO. The precipitate and the film prepared through the liquid-crystalline state exhibited the exothermic transition at 160 °C by DSC. The diffraction pattern of the film annealed at 200 °C is shown in Figure 3. A meridional reflection was also observed at 1.42 Å. The reflection spacings were explained by an orthorhombic unit cell which is nearly isometric to that of PClBO (Table I). The ω-form of PBrBO was considered to be stable, since the reverse transition from ω to α was not observed in spite of our various attempts. As in the case of PClBO, the film dried quickly from the dilute solution did not exhibit the exothermic transition, and the diffraction pattern remained broad, while the IR data supported the conformational transition.

These results for PXBO's are summarized as follows. The molecular conformation in the films as cast is α-helical. Heat treatments cause the transition at ~160 °C into the ω-helix for PFBO, PClBO, and PBrBO. The orthorhombic crystal structures are considered to be isomorphous. The space group is presumably $P2_12_12_1$-D_2^4 from the absences of the $h00$ reflections with $h \neq 2n$ and the $0k0$ reflections with $k \neq 2n$. This suggests that even if the main chain assumes the 4-fold helix, the entire helix including the side chains has only 2_1 symmetry; i.e., the side-chain conformations should not be unique.

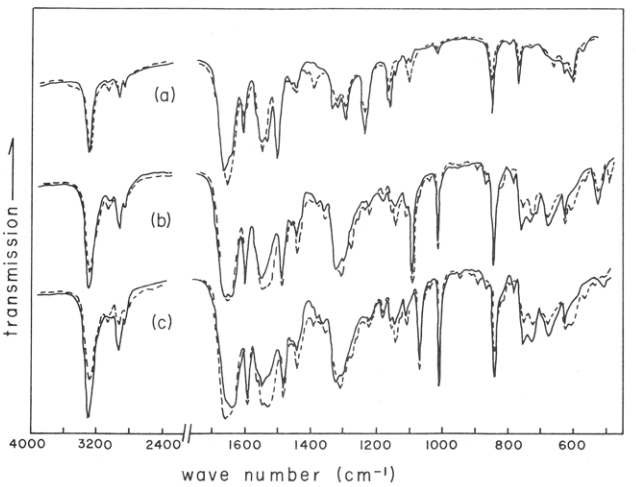

Figure 4. Infrared spectra of (a) the α-form (---) and the ω-form (—) of PFBO and polarized infrared spectra of the ω forms of (b) PClBO and (c) PBrBO. For (b) and (c), (—) electric vector is parallel to the fiber axis, (---) electric vector is perpendicular to the fiber axis.

Infrared Spectroscopy. Figure 4 shows the IR spectra of the α- and ω-forms of PFBO and the polarized spectra of the ω forms of PClBO and PBrBO. The spectral change by the α → ω transition has the following features. First, the frequency shifts of the characteristic absorptions were small (Table II). This suggests that the conformational difference between α and ω is small and/or that the absorptions of the main-chain and side-chain amide groups are overlapped. Second, some sharp bands appeared, while the broad absorption at ~3400 cm^{-1} assigned to the stretching vibration of free N–H groups disappeared. This indicates that the side chains in the ω-forms are completely hydrogen bonded and incorporated into the crystalline order.

The orientation of atomic groups with respect to the helix axis has been investigated by dichroism measurements for esters of poly(L-glutamic acid).[16-19] We may use this technique[3,15] for the ω forms of PClBO and PBrBO

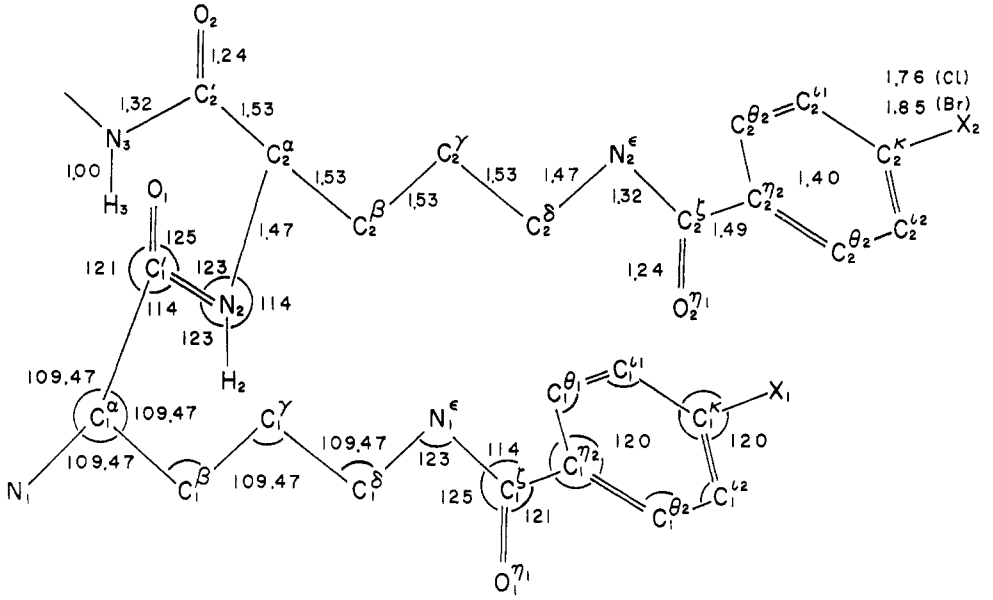

Figure 5. Designation of atoms, bond lengths (upper, in Å), and bond angles (lower, in deg) used in this work. The main-chain dimensions are those of Corey and Pauling[13] except $\tau(N,C^{\alpha},C') = 109.47°$.

Table III
Orientation of Direction Normal to *p*-Halophenyl Planes

method		direction angle θ, deg	
		PClBO	PBrBO
IR		51	48
X-ray	residue 1	56	55
	residue 2	49	47

in order to determine the orientation of the side-chain end groups. The *p,p'*-disubstituted phenyl group has C_{2v} symmetry. Its infrared-active local vibrations are classified into three types, A_1, B_1, and B_2. The direction of the transition moments are along the C_2 symmetry axis (A_1), perpendicular to the phenyl ring (B_2), and perpendicular to these two axes (B_1). In poly(γ-benzyl-L-glutamate), the bands at 1498 and 1453 cm^{-1} were assigned to C–C stretching vibrations of A_1 and B_1 modes, respectively.[16] The corresponding bands were probably the bands at 1488 and 1442 cm^{-1} (PClBO) and at 1481 and 1440 cm^{-1} (PBrBO). It was suggested, however, that they overlapped possibly with absorptions of other atomic groups.[16] Even by referring to the spectroscopic data of low molecular weight compounds,[20,21] the assignment of the bands at 1092 and 1013 cm^{-1} (PClBO) and at 1069 and 1011 cm^{-1} (PBrBO) were not clear (possibly in-plane C–H bending or C–C–C bending). The bands at 757 cm^{-1} (PClBO) might be assigned to C–Cl stretching (A_1), but this seemed to overlap with other absorptions. If this band were uniquely attributed to C–Cl stretching, the corresponding C–Br stretching would appear in the lower frequency region. A band was, however, observed at a similar frequency 752 cm^{-1} for PBrBO. Finally, the sharp bands at 845 (PClBO) and 840 cm^{-1} (PBrBO) were assigned to out-of-plane C–H bending (B_2) and regarded to be free from overlapping. The direction angles evaluated by eq 3 are listed in Table III. These values are comparable with the results by X-ray analysis.

Main-Chain Structure. The ω-helix with $p = 1.42$ Å is not described by the conventional ribbon model, as described before. A question arises whether such a helix is geometrically possible or not. The uniform helix has three independent torsion angles, namely, $\phi(N-C^{\alpha})$, $\psi(C^{\alpha}-C')$, and $\omega(C'-N)$. The two conditions of $p = 1.42$ Å and $t = 90°$ leave one degree of freedom. We adopted here the Corey–Pauling dimensions and $\tau(N,C^{\alpha},C') = 109.47°$ for the backbone chain (Figure 5). The assumption of $\omega = 180$ yields $\phi = -29.3°$ and $\psi = -85.5°$, but these angles do not seem to be acceptable. Then, the out-of-plane deformation of the peptide unit was taken into account. The hydrogen-bond distance $b(N_5,O_1)$, its angle $\tau(H_5,N_5,O_1)$, ϕ, and ψ are plotted in Figure 6 as functions of ω. The model with $\omega = 186°$ was judged to be most favorable, since the parameters $\phi = -54.2°$, $\psi = -61.6°$, $b(N_5,O_1) = 2.89$ Å, and $\tau(H_5,N_5,O_1) = 16.2°$ are comparable to those of the standard α-helix. The empirical conformational energies were calculated[22] for a chain consisting of L-alanyl residues by using essentially the same parameters as in ECEPP.[23] The energies are also plotted in Figure 6, where the minimum is observed at $\omega \sim 186°$. The torsion angle ω was adjusted in the refinement of the following X-ray analysis, and the value 186° was actually found to be most probable.

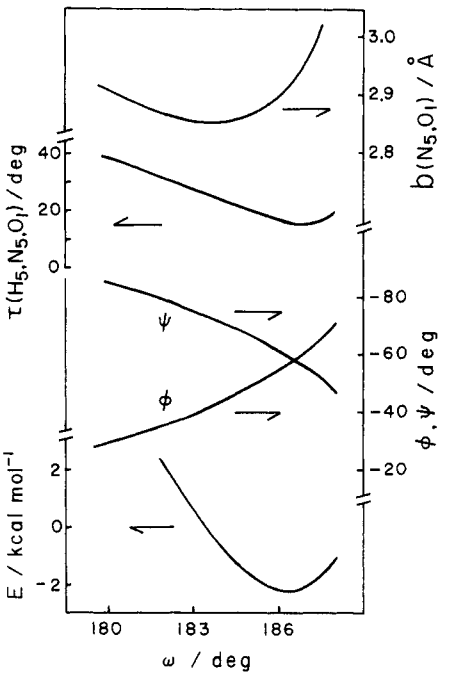

Figure 6. ω-Dependence of $b(N_5,O_1)$, $\tau(H_5,N_5,O_1)$, ϕ, ψ, and the conformation energy E (kcal/mol of residue) calculated for the right-handed helix with $p = 1.42$ Å and $t = 90°$.

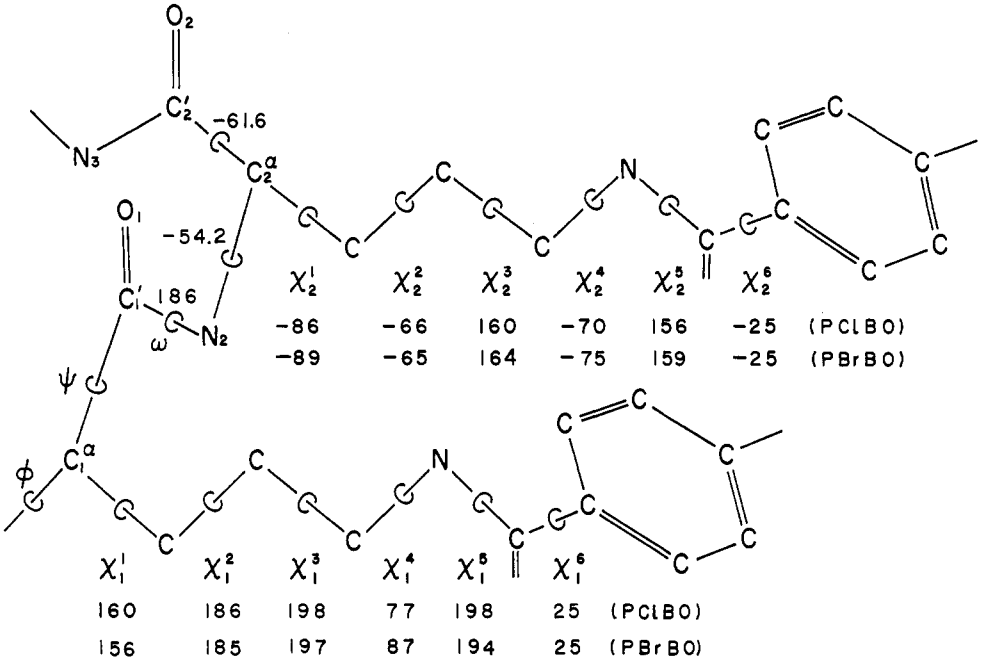

Figure 7. Torsion angles in the ω-forms of PClBO and PBrBO.

Crystal Structure. The ω-forms of PClBO and PBrBO offered the well-defined diffraction data. It was necessary, however, to reduce the number of structural parameters by employing the linked-atom least-squares method (LALS), in which the bond lengths and the bond angles were constrained to their standard values given in Figure 5. The LALS technique[24] has been used in the analyses of many biological[10,24-27] and synthetic polymers,[28-30] and its usefulness is generally recognized.

The structure of PBrBO was analyzed first, since it contains the heavier atom Br, useful for the structure determination. The structure of $P2_12_12_1$ projected along the c axis has a center of symmetry. Therefore, the structure factors of the equatorial reflections can be given by real quantities. If their phase factors (+1 or −1) are determined, we can calculate the equatorial electron-density projection. By making use of this property, the structure was analyzed in the following procedure.

The LALS refinements were performed for the molecular models with various side-chain conformations. The χ^5 for the side-chain amide group (Figure 7) was assumed to be 180° (*trans*) in the earlier stage, but it was finally adjusted. There are two factors governing the torsion angle χ^6. One is the tendency to keep the coplanarity of the phenyl ring and the side-chain amide plane owing to the partial double-bond character. The other is the steric hindrance between the ortho-positioned hydrogen atom of the phenyl group and the oxygen atom of the amide group. It was shown that the conformational energy became minimum at χ^6 = 25° in aromatic polyamides.[31] Then, the χ^6 was fixed at either 25° or −25°. The intensities (I_c's) were calculated by neglecting the hydrogen atoms and by assuming the appropriate temperature factors listed in Table IV. The electron-density map was calculated from the observed intensity data (I_o's) by using the phase factors of the LALS result. The map was naturally incomplete (partly false) but offered the position of the heavy atom. After modifying the model, the LALS refinements were continued.

In the refinement procedure, it was clarified that the side chains take two distinctive conformations alternately in accord with the 2_1 symmetry of the crystal. Therefore, four combinations arise for χ_1^6 and χ_2^6 of the consecutive side chains (±25°, ±25°). Furthermore, the amide groups of the side chains differing in conformation approach each other so that they are able to form intra- and intermolecular hydrogen bonds. Their distances b(N,O) were adjusted in the range from 2.8 to 2.9 Å. The refined parameters were the main-chain torsion angle ω, 10 torsion angles of the consecutive side chains (χ_1^1 to χ_1^5 and χ_2^1 to χ_2^5) (Figure 7), the axial translation of the helix, and the ro-

Table IV
Atomic Coordinates and Temperature Factors of the ω-Form of PBrBO

atom	x	y	z	temperature factor, Å^2
N_1	0.022	−0.092	−0.300	5.0
C_1^{α}	0.071	−0.096	−0.152	5.0
C'_1	0.069	−0.037	0.036	5.0
O_1	0.068	−0.052	0.248	5.0
N_2	0.069	0.030	−0.050	5.0
C_2^{α}	0.072	0.095	0.098	5.0
C'_2	0.028	0.092	0.286	5.0
O_2	0.039	0.091	0.498	5.0
C_1^{β}	0.122	−0.086	−0.304	5.0
C_1^{γ}	0.169	−0.059	−0.151	7.0
C_1^{δ}	0.218	−0.043	−0.307	10.0
N_1^{ϵ}	0.267	−0.038	−0.160	15.0
C_1^{ζ}	0.297	−0.096	−0.105	15.0
$O_1^{\eta 1}$	0.293	−0.156	−0.200	15.0
$C_1^{\eta 2}$	0.336	−0.082	0.090	15.0
$C_1^{\theta 1}$	0.326	−0.027	0.254	15.0
$C_1^{\theta 2}$	0.383	−0.125	0.108	15.0
$C_1^{\iota 1}$	0.363	−0.015	0.436	15.0
$C_1^{\iota 2}$	0.420	−0.113	0.290	15.0
C_1^{κ}	0.410	−0.058	0.455	15.0
Br_1	0.459	−0.041	0.696	20.0
C_2^{β}	0.065	0.163	−0.054	5.0
C_2^{γ}	0.120	0.188	−0.147	7.0
C_2^{δ}	0.155	0.212	0.059	10.0
N_2^{ϵ}	0.212	0.216	−0.017	15.0
C_2^{ζ}	0.243	0.158	−0.051	15.0
$O_2^{\eta 1}$	0.234	0.097	0.035	15.0
$C_2^{\eta 2}$	0.291	0.171	−0.205	15.0
$C_2^{\theta 1}$	0.290	0.227	−0.369	15.0
$C_2^{\theta 2}$	0.337	0.126	−0.184	15.0
$C_2^{\iota 1}$	0.335	0.239	−0.514	15.0
$C_2^{\iota 2}$	0.382	0.138	−0.329	15.0
C_2^{κ}	0.381	0.195	−0.493	15.0
Br_2	0.441	0.210	−0.685	20.0

Table V
Comparison between Observed and Calculated Intensities of the ω-Form of PBrBO

hkl	$I_o^{1/2}$	$I_c^{1/2}$	hkl	$I_o^{1/2}$	$I_c^{1/2}$
110	148	106	101	117	135
200	291	198	011	0	25
210	99	77	111, 201	275	304
020	168	158			
120	0	10	211	0	83
310, 220	232	223	021, 121, 301	250	220
400, 320	112	54	311, 221	320	246
130	0	43			
410	171	129	401, 031, 321, 131	364	363
230	209	249			
420	156	99			
330	83	100			
510	87	80	411		
040, 140	579	465	231	0	99
			421	156	228
430, 520, 240	220	269	501, 331	0	89
			511	0	43
600, 340, 610	392	379	041, 141	370	250
			431, 521, 241	383	459
530	126	68			
620, 440	0	15	601	0	50
150	295	292	341, 611	162	200
250	0	2			
710	0	75	531	0	73
630, 540, 350	379	407	621	0	21
			441, 051	175	204
720	0	44	151		
450	0	40	251, 701	0	69
800, 640, 060, 730, 160	278	301	711, 631	200	205

tation about the axis. Since only 29 reflections were observed, 16 missing reflections were included in the LALS refinement as they had the structure factors of zero magnitudes. The total number of the reflection data (45) was considered to be enough in contrast to the number of the parameters, although we must allow the large standard deviations. Refining the temperature factors is meaningless in the present case.

A good result was obtained when the side-chain hydrogen-bond distance b(N,O) = 2.85 Å, $\chi_1^6 = +25°$, and $\chi_2^6 = -25°$. The discrepancy factor $R = \sum(I_o^{1/2} - I_c^{1/2})/\sum I_o^{1/2}$ was reduced to 17% for the observed reflections and 29% for the total data. Although the R factor was rather insensitive to the change of ω, it took the minimum value at $\omega = 186°$. The atomic fractional coordinates of the most probable structure and the assumed temperature factors are listed in Table IV. The observed and calculated intensities are compared in Table V. The torsion angles are given in Figure 7. The electron-density map projected (averaged) along the c axis is shown in Figure 8, on which the molecular backbones are superimposed. The molecular structure is illustrated in Figure 9. The orientation of the direction normal to the p-halophenyl plane was calculated from the atomic coordinates (Table III). The discrepancy between the results by IR and X-ray analyses are within the experimental error of both methods.

According to the same procedure, the structure of the ω-form of PClBO was found to be isomorphous. The torsion angles are essentially the same as those of PBrBO (Figure 7). The side-chain hydrogen-bond distance was adjusted to 2.86 Å to reduce the R factor, which was 22% for the 24 observed reflections (38% for the 40 reflections including the missing ones).

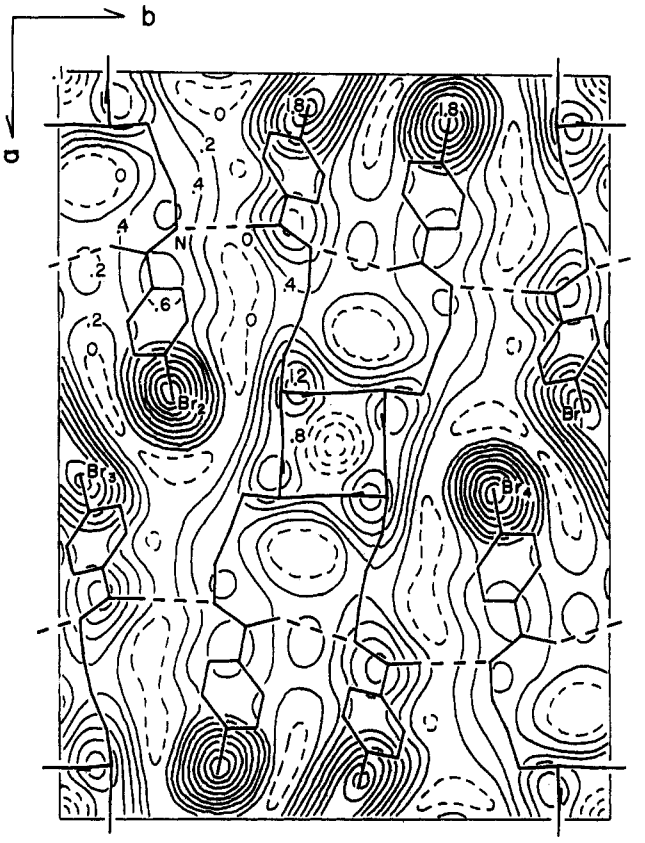

Figure 8. Electron-density map of the equatorial projection of the ω-form of PBrBO superimposed with the molecular backbones. Side-chain hydrogen bonds are shown by broken lines. The figures are in units of electrons Å^{-3}. Contours are at intervals of 0.2 electrons Å^{-3}.

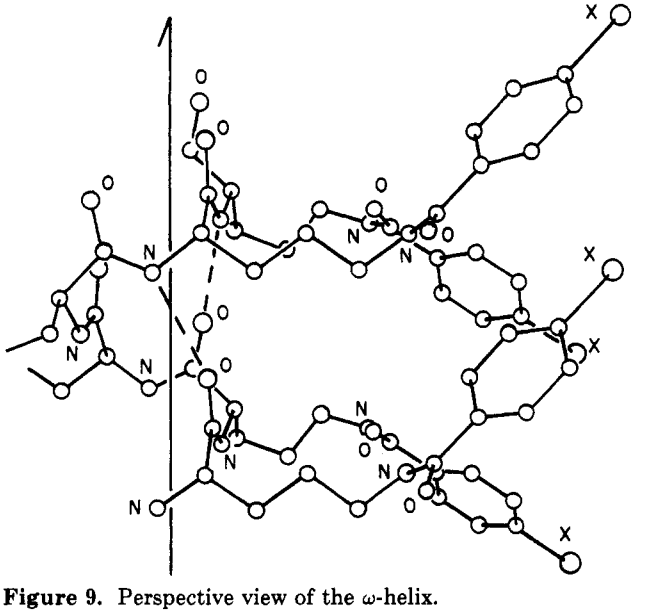

Figure 9. Perspective view of the ω-helix.

Discussion and Conclusions

The ω-forms found for PXBO's with X = F, Cl, and Br are characterized as follows.

(1) The unit height p = 1.42 Å is beyond the scope of the ribbon model. This is discussed below.

(2) These ω-forms crystallize in the isomorphous orthorhombic structure with space group $P2_12_12_1$-D_2^4. The side chains take two distinctive conformations alternately

in accord with the crystal symmetry.

(3) Intra- and intermolecular hydrogen bonds are formed between the amide groups of the side chains differing in the conformation. The disordered molecular packing persisted even by heat treatments in the films of PClBO and PBrBO prepared by drying quickly the dilute solutions. The diffraction pattern is not of the ω-form, but the IR data supported the ω-helical conformation. The random orientation of the rodlike molecules as in the isotropic solution might be fixed by the side-chain hydrogen bonding.

(4) As inferred from the transition behavior, the stability of the ω-helices increases in the order PFBO < PClBO < PBrBO. Recently, we synthesized the polymers with X = p-CH_3 and m-Br. The ω structure was observed for the former but not for the latter.[22] This indicates that the existence of the large atom (or group) at the para position is important. As shown in Figure 8, the halogen atoms lie close together. In the most probable structure, Cl_1–Cl_3, = 3.78 Å, Cl_2–$Cl_{3'}$ = 4.02 Å, Br_1–$Br_{3'}$ = 3.80 Å, and Br_2–$Br_{3'}$ = 4.02 Å. If the para-substituted atom is small, the unit-cell *a* dimension may become smaller so as to break the intermolecular hydrogen bonds.

(5) The C_6H_4X groups are bulky and stacked to each other; the van der Waals diameters of Cl (3.6 Å) and Br atoms (3.9 Å) are comparable to the thickness of the phenyl ring (3.70 Å). Furthermore, the side chains are hydrogen bonded. Accordingly, the side-chain motions should be strongly prohibited. This is consistent with the concentrated appearance of the halogen atoms in the electron-density map (Figure 8). Only feasible is the wiggling and/or the hindered rotation of the phenyl groups about the C_2 symmetry axis as in polycarbonates,[32] i.e., the motions about the torsion angle χ^6. The final *R* factor was 3–5% smaller for the case of $\chi_1^6 = +25°$ and $\chi_2^6 = -25°$ than for other three cases. But the difference is not decisive. It is considered that some wiggling or rotational motions of phenyl groups take place cooperatively among neighboring groups. In fact, the phenyl groups are not resolved well in the electron-density map.

The Ribbon Model. The present ω-helix deviates fairly from the ribbon model (Figure 1). However, this helical structure is realized by the out-of-plane deformation of the peptide unit. The nonplanar peptide unit has been observed for the ω-helices. The left-handed ω-helix of PBLA assumed ω = 175°.[4] The ω-helix of p-Cl-PBLA was shown to have a relatively low conformational energy despite the nonplanar peptide unit.[33] A δ-helical (4_{14}) structure with the hydrogen bonding of the (N_1—H_1···O_4=C_4') type was proposed for PBLA by allowing the out-of-plane deformation,[34] but it has not yet been established.

With respect to the ribbon model, a question arises why the unit heights of the α-helices fall in the small range 1.47–1.525 Å,[1-3] while the ω-helices are dispersed in the range *p* = 1.30–1.42 Å. In order to understand this, the conformational energy calculations are necessary.[22] In this work, we surveyed the molecular models geometrically under the criteria (1) φ and ψ = −45° to −75°, (2) $b(N_5,O_1)$ = 2.84 to 2.92 Å, and (3) $\tau(H_5,N_5,O_1) < 30°$. The hydrogen-bond distances of the α- and ω-helices are confined in this range.[3] When ω = 180°, the α-helices can exist with *p* = 1.49–1.52 Å, while the ω-helices are impossible. When we permit the nonplanar deformation of the peptide units, the ω-helices become possible with *p* = 1.29–1.44 Å. Therefore, the unit heights of p-ClPBLA (1.30 Å)[5] and PXBO's (1.42 Å) are virtually the lower and upper limits, respectively. On the other hand, the unit heights of the α-helices are still in the range 1.48–1.52 Å with the nonplanar peptide units.

It is thus important to take into account the out-of-plane deformation of the peptide unit. We must employ the ribbon model carefully. In this connection, Figure 1 should be replaced by the map in which the potential energies minimized with the torsion angle ω are plotted against *p* and *t*. The results of energy calculations will be reported in the forthcoming publication.[22]

Registry No. PHBO (homopolymer), 108317-44-8; PHBO (SRU), 108334-85-6; PFBO (homopolymer), 115962-04-4; PFBO (SRU), 115962-09-9; PClBO (homopolymer), 115962-06-6; PClBO (SRU), 115962-10-2; PBrBO (homopolymer), 115962-08-8; PBrBO (SRU), 115962-11-3.

References and Notes

(1) Bamford, C. H.; Elliott, A.; Hanby, W. E. *Synthetic Polypeptides*; Academic: New York, 1956.
(2) *Poly-α-Amino Acids*; Fasman, G. D., Ed.; Marcel Dekker: New York, 1967.
(3) Fraser, R. D. B.; MacRae, T. P. *Conformation in Fibrous Proteins*; Academic: New York, 1973.
(4) Bradbury, E. M.; Brown, L.; Downie, A. R.; Elliott, A.; Fraser, R. D. B.; Hanby, W. E. *J. Mol. Biol.* **1962**, *5*, 230.
(5) Takeda, Y.; Iitaka, Y.; Tsuboi, M. *J. Mol. Biol.* **1970**, *51*, 101.
(6) Fraser, R. D. B.; MacRae, T. P.; Stapleton, I. W. *Nature (London)* **1962**, *193*, 573.
(7) Yamashita, O.; Yamane, T.; Asada, T.; Yamashita, S.; Yamashita, T. *Polym. J. (Tokyo)* **1979**, *11*, 763.
(8) Kōmoto, T.; Kodaka, M.; Kawai, T. *Makromol. Chem.* **1979**, *180*, 819.
(9) Sasaki, S.; Yasumoto, Y.; Uematsu, I. *Macromolecules* **1981**, *14*, 1797.
(10) Malcolm, B. R.; Walkinshaw, M. D. *Biopolymers* **1986**, *25*, 607.
(11) Toniolo, C.; Bonora, G. M.; Bavoso, A.; Benedetti, E.; Di Blasio, B.; Pavone, V.; Pedone, C. *Macromolecules* **1986**, 19, 472.
(12) Fraser, R. D. B.; Harrap, B. S.; Ledger, R.; MacRae, T. P.; Stewart, C.; Suzuki, E. *Biopolymers* **1967**, *5*, 797.
(13) Corey, R. B.; Pauling, L. *Proc. R. Soc. London, B* **1953**, *141*, 10.
(14) Leach, S. J.; Némethy, G.; Scheraga, H. *Biopolymers* **1966**, *4*, 369.
(15) Fraser, R. D. B. *J. Chem. Phys.* **1953**, *21*, 1511.
(16) Tsuboi, M. *J. Polym. Sci.* **1962**, *59*, 139.
(17) Delporte-Leroy, M.; Le Barny, P.; Loucheux-Lefebvre, M. H. *Macromolecules* **1973**, *6*, 780.
(18) Tanaka, A.; Ishida, Y. *J. Polym. Sci., Polym. Phys. Ed.* **1973**, *11*, 1117.
(19) Iizuka, E. *Polym. J. (Tokyo)* **1975**, *7*, 650.
(20) Bellamy, L. J. *The Infrared Spectra of Complex Molecules*; Chapman and Hall: London, 1975.
(21) Colthup, N. B.; Wiberley, S. E.; Daly, L. H. *Introduction to Infrared and Raman Spectroscopy*; Academic: New York, 1975.
(22) Sasaki, S., in preparation.
(23) Momany, F. A.; McGuire, R. F.; Burgess, A. W.; Scheraga, H. A. *J. Phys. Chem.* **1975**, *79*, 2361.
(24) Arnott, S.; Wonacott, A. J. *Polymer* **1966**, *7*, 157.
(25) Arnott, S.; Wonacott, A. J. *J. Mol. Biol.* **1966**, *21*, 371.
(26) Arnott, S.; Dover, S. D.; Wonacott, A. J. *Acta Crystallogr., Sect. B: Struct. Crystallogr. Cryst. Chem.* **1969**, *B25*, 2192.
(27) Arnott, S.; Selsing, E. *J. Mol. Biol.* **1974**, *88*, 509.
(28) Sasaki, S.; Takahashi, Y.; Tadokoro, H. *J. Polym. Sci., Polym. Phys. Ed.* **1972**, *10*, 2363.
(29) Takahashi, Y.; Tadokoro, H. *Macromolecules* **1973**, *6*, 672.
(30) Takahashi, Y.; Sato, T.; Tadokoro, H.; Tanaka, Y. *J. Polym. Sci., Polym. Phys. Ed.* **1973**, *11*, 233.
(31) Tashiro, K.; Kobayashi, M.; Tadokoro, H. *Macromolecules* **1977**, *10*, 413.
(32) Schaefer, J.; Stejskal, E. O.; Perchak, D.; Skolnick, J.; Yaris, R. *Macromolecules* **1985**, *18*, 368.
(33) Fu, Y.-C.; McGuire, R. F.; Scheraga, H. A. *Macromolecules* **1974**, *7*, 468.
(34) Nambudripad, R.; Bansal, M.; Sasisekharan, V. *Int. J. Pept. Protein Res.* **1981**, *18*, 374.